Gamma Guidance of Trajectories for Coplanar, Aeroassisted Orbital Transfer

A. Miele* and T. Wang†
Rice University, Houston, Texas 77251

This paper is concerned with the optimization and guidance of trajectories for coplanar, aeroassisted orbital transfer from high Earth orbit to low Earth orbit. Optimal trajectories are computed by minimizing the total velocity impulse required for orbital transfer. They include two branches: a relatively short descending flight branch (branch 1) and a long ascending flight branch (branch 2). Near-optimal guidance trajectories are implemented via a feedback control scheme in which the lift coefficient is adjusted according to a two-stage gamma guidance law. For branch 1, the gamma guidance is a linear path inclination guidance; for branch 2, the gamma guidance is a constant path inclination guidance. A modified gamma guidance is developed; it differs from the gamma guidance in two aspects: lower target altitude and use of a predictor-corrector algorithm to determine the switch velocity and the target path inclination. The modified gamma guidance is quite stable with respect to dispersion effects arising from navigation errors, variations of the atmospheric density, and uncertainties in the aerodynamic coefficients.

Nomenclature

C_D = drag coefficient
C_{D0} = zero-lift drag coefficient
C_L = lift coefficient
D = drag, N
F = dispersion factor
g = local acceleration of gravity, m/s^2
H = $r_a - r_e$ = thickness of the atmosphere, m
HR = heating rate, W/m^2
h = altitude, m
K = induced drag factor
L = lift, N
m = mass, kg
PHR = peak heating rate, W/m^2
r = radial distance from the center of the Earth, m
r_e = radius of the Earth, m
r_a = radius of the outer edge of the atmosphere, m
S = reference surface area, m^2
T = running time, s
t = T/τ = dimensionless time
V = velocity, m/s
V_a = $\sqrt{\mu/r_a}$ = circular velocity at $r = r_a$, m/s
γ = path inclination, rad
μ = Earth's gravitational constant, m^3/s^2
ρ = air density, kg/m^3
τ = final time, s
ΔV = characteristic velocity, m/s

Subscripts

0 = entry into the atmosphere
1 = exit from the atmosphere
00 = exit from the initial orbit
11 = entry into the final orbit

Superscripts

$'$ = derivative with respect to dimensionless time
$\sim$ = condition following the application of a velocity impulse or nominal condition

Received March 15, 1990; portions of this paper were presented as ICAS Paper 90-151 at the 17th Congress of the International Council of the Aeronautical Sciences, Stockholm, Sweden, Sept. 9-14, 1990; revision received Oct. 12, 1990; accepted for publication Oct. 21, 1990.

*A. J. Foyt Family Professor in Engineering and Professor of Aerospace Sciences and Mathematical Sciences, Aero-Astronautics Group. Fellow AIAA.

†Senior Research Scientist, Aero-Astronautics Group. Senior Member AIAA.

I. Introduction

SAVING propellant weight and increasing the payload are among the most important problems of space transportation. Orbital transfer from high Earth orbit (HEO) to low Earth orbit (LEO) can be made more economic if the aeroassisted orbital transfer (AOT) mode is employed. In the AOT mode, use is made of the aerodynamic forces to achieve the proper amount of velocity depletion during the atmospheric pass. The intent is to achieve a specified apogee following the atmospheric exit, while minimizing the overall propellant consumption and keeping the peak heating rate within reasonable bounds during the atmospheric pass.

Aeroassisted orbital transfer is not only important for HEO-to-LEO transfer maneuvers but may prove to be indispensable for future planetary flights. In particular, this statement refers to lunar return vehicles, Mars exploration vehicles, and Mars return vehicles.

Over the past several years, considerable research has been done on two aspects of coplanar, aeroassisted orbital transfer: trajectory optimization[1-5] and trajectory guidance.[6-10] In particular, in Ref. 10, a two-stage guidance scheme, consisting of the combination of target altitude guidance and target path inclination guidance, was developed for the atmospheric pass of an AOT spacecraft, akin to the target altitude guidance already developed for the abort landing of an aircraft in a windshear.[11]

This paper continues the work of Ref. 10. Starting from the study of the optimal trajectories, it develops a near-optimal, two-stage gamma guidance, akin to the gamma guidance already developed for the abort landing of an aircraft in a windshear.[12] Also, a modified gamma guidance is developed to improve the stability with respect to dispersion effects arising from navigation errors, variations of the atmospheric density, and uncertainties in the aerodynamic coefficients.

II. System Description

We consider coplanar, aeroassisted orbital transfer from high Earth orbit to low Earth orbit. We employ the following

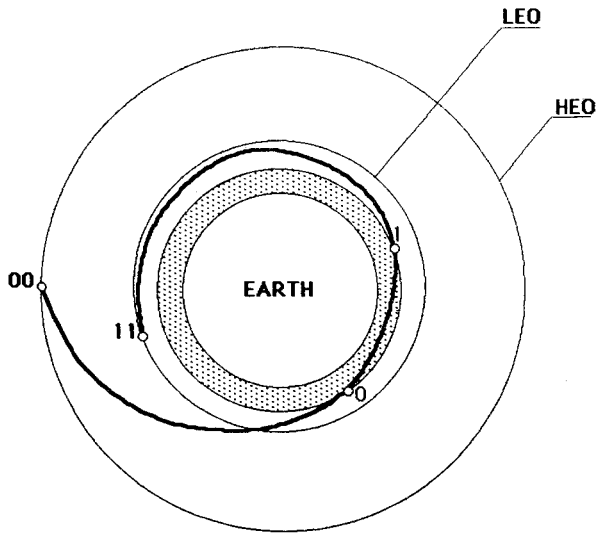

Fig. 1 Coplanar, aeroassisted orbital transfer.

assumptions: 1) the initial and final orbits are circular; 2) three impulses are employed, one at the exit from the initial orbit, one at the exit from the atmosphere, and one at the entry into the final orbit; and 3) the gravitational field is central and is governed by the inverse square law. The four key points of the maneuver are these: point 00, exit from the initial orbit; point 0, entry into the atmosphere; point 1, exit from the atmosphere; and point 11, entry into the final orbit; see Fig. 1.

The maneuver starts in high Earth orbit with a tangential propulsive burn, having characteristic velocity ΔV_{00}, at point 00; here, the spacecraft enters into an elliptical transfer orbit, connecting the points 00 and 0; this elliptical transfer orbit is such that its apogee occurs at r_{00}. At point 0, the spacecraft enters into the atmosphere; after traversing the upper layers of the atmosphere, it exits from the atmosphere at point 1; during the atmospheric pass, the velocity of the spacecraft is depleted, due to the aerodynamic drag. At point 1, the maneuver continues with a tangential propulsive burn, having characteristic velocity ΔV_1; then the spacecraft enters into an elliptical transfer orbit connecting the points 1 and 11; this elliptical transfer orbit is such that its apogee occurs at r_{11}. The maneuver ends with a tangential propulsive burn, having characteristic velocity ΔV_{11}, at point 11; here, the spacecraft enters into the low Earth orbit, in that the magnitude of ΔV_{11} is such that the desired circularization into LEO is achieved.

A. Atmospheric Pass

For the atmospheric portion of the trajectory of the AOT vehicle, we employ the following hypotheses: 1) the atmospheric pass is made with the engine shut off; hence, in this portion of the flight, the AOT vehicle behaves as a particle of constant mass; 2) Coriolis acceleration terms and transport acceleration terms are neglected; 3) the spacecraft is controlled via the lift coefficient; 4) the aerodynamic forces are evaluated using the inertial velocity rather than the relative velocity; and 5) under extreme hypersonic conditions, the dependence of the aerodynamic coefficients on the Mach number and the Reynolds number is disregarded.

B. Differential System

With the above assumptions, and upon normalizing the flight time to unity, the equations of motion are given by

$$\dot{h} = \tau[V \sin\gamma] \tag{1a}$$

$$\dot{V} = \tau[-D/m - g \sin\gamma] \tag{1b}$$

$$\dot{\gamma} = \tau[L/mV + (V/r - g/V) \cos\gamma] \tag{1c}$$

with $0 \leq t \leq 1$. In the above equations,

$$r = r_e + h, \qquad g = \mu/r^2 = \mu/(r_e + h)^2 \tag{2}$$

In addition, the aerodynamic forces are given by

$$D = \tfrac{1}{2} C_D \rho S V^2, \qquad L = \tfrac{1}{2} C_L \rho S V^2 \tag{3a}$$

with $\rho = \rho(h)$. In particular, if a parabolic polar is postulated, the relation between the drag coefficient and the lift coefficient is given by

$$C_D = C_{D0} + K C_L^2 \tag{3b}$$

C. Control Constraint

To obtain realistic solutions, the presence of upper and lower bounds on the lift coefficient is necessary. Therefore, the two-sided inequality constraint

$$C_{La} \leq C_L \leq C_{Lb} \tag{4}$$

must be satisfied everywhere along the interval of integration.

D. Boundary Conditions

At the entry into the atmosphere ($t = 0$) and at the exit from the atmosphere ($t = 1$), certain static and dynamic boundary conditions must be satisfied. Specifically, at atmospheric entry, we have

$$h_0 = H \tag{5a}$$

$$r_{00}^2(2V_a^2 - V_0^2) - 2r_{00}r_a V_a^2 + r_a^2 V_0^2 \cos^2\gamma_0 = 0 \tag{5b}$$

In addition, at atmospheric exit, we have

$$h_1 = H \tag{6a}$$

$$r_{11}^2(2V_a^2 - \tilde{V}_1^2) - 2r_{11}r_a V_a^2 + r_a^2 \tilde{V}_1^2 \cos^2\gamma_1 = 0 \tag{6b}$$

Because the velocity impulse ΔV_1 is applied at atmospheric exit, the following relation holds:

$$\Delta V_1 = \tilde{V}_1 - V_1 \tag{7a}$$

where V_1 and $\tilde{V}_1$ denote the values of the exit velocity before and after the application of the propellant burn. In light of Eq. (6b), the value of the exit velocity after the application of the propellant burn can be written as

$$\tilde{V}_1 = V_a \sqrt{2(r_{11}^2 - r_{11}r_a)/(r_{11}^2 - r_a^2 \cos^2\gamma_1)} \tag{7b}$$

E. Experimental Data

The following data are used in the numerical experiments for optimal trajectories and guidance trajectories.

Spacecraft

For the spacecraft, it is assumed that the mass per unit reference surface area is $m/S = 300$ kg/m^2; the zero-lift drag coefficient is $C_{D0} = 0.1$; the induced drag factor is $K = 1.11$; the lift coefficient for maximum lift-to-drag ratio is $C_{LE} = 0.3$; the maximum lift-to-drag ratio is $E_{\max} = 1.5$; and the bounds on the lift coefficient are $C_{La} = -0.9$ and $C_{Lb} = +0.9$.

Physical Constants

The major physical constants used in the computations are as follows: the radius of the Earth is $r_e = 6378$ km; the radius of the outer edge of the atmosphere is $r_a = 6498$ km; the thickness of the atmosphere is $H = 120$ km; and the Earth's gravitational constant is $\mu = 0.3986E + 06$ km^3/s^2.

Transfer Maneuvers

Three transfer maneuvers are considered, involving different values of the HEO radius, but the same value of the LEO radius. To describe these maneuvers, let α and β denote the dimensionless ratios

$$\alpha = r_{00}/r_a, \qquad \beta = r_{11}/r_a \tag{8}$$

Case 1. The HEO radius is $r_{00} = 12{,}996$ km, $\alpha = 2$. The LEO radius is $r_{11} = 6558$ km, $\beta = 1.00923$.

Case 2. The HEO radius is $r_{00} = 25{,}992$ km, $\alpha = 4$. The LEO radius is $r_{11} = 6558$ km, $\beta = 1.00923$.

Case 3. The HEO radius is $r_{00} = 42{,}164$ km, $\alpha = 6.48877$. The LEO radius is $r_{11} = 6558$ km, $\beta = 1.00923$. Here, HEO = GEO.

Atmospheric Model

The atmospheric model assumed is that of the US Standard Atmosphere, 1976 (Ref. 13).

Heating Rate

The heating rate HR is computed with the relation

$$HR = C\sqrt{\rho/\rho_R}\,(V/V_R)^{3.08} \tag{9}$$

Here, $\rho_R = 0.39957E-02$ kg/m^3 is a reference density (density at the reference altitude $h_R = 40$ km) and $V_R = V_a = 7.832$ km/s is a reference velocity. The constant C represents the heating rate at $V = V_R$ and $h = h_R$; its value is assumed to be $C = 348.7$ W/cm^2.

III. Optimal Trajectories

A. Performance Index

Subject to the previous constraints, different AOT optimization problems can be formulated, depending on the performance index chosen. The resulting optimal control problems are either of the Bolza type or of the Chebyshev type. In this paper, only one performance index is considered, the minimum energy required for orbital transfer. A measure of this energy is the total characteristic velocity ΔV, the sum of the characteristic velocity ΔV_{00} associated with the propulsive burn from the initial orbit, the characteristic velocity ΔV_1 associated with the propulsive burn at the exit of the atmosphere, and the characteristic velocity ΔV_{11} associated with the propulsive burn into the final orbit. Clearly,

$$I = \Delta V = \Delta V_{00} + \Delta V_1 + \Delta V_{11} \tag{10a}$$

with

$$\Delta V_{00} = \sqrt{r_a/r_{00}}\,V_a - (r_a/r_{00})V_0\cos\gamma_0 \tag{10b}$$

$$\Delta V_1 = \tilde{V}_1 - V_1 \tag{10c}$$

$$\Delta V_{11} = \sqrt{r_a/r_{11}}\,V_a - (r_a/r_{11})\tilde{V}_1\cos\gamma_1 \tag{10d}$$

In the last two equations, $\tilde{V}_1$ is supplied by Eq. (7b).

B. Numerical Results

Optimal trajectories were computed by minimizing the performance index (10), subject to the constraining relations. Three transfer maneuvers were considered; see cases 1, 2, and 3 of Sec. II. The sequential gradient-restoration algorithm was employed in primal form.[14-16] This is a first-order algorithm that generates a sequence of feasible solutions, each characterized by a lower value of the performance index (10). The numerical results are shown in Table 1 and Fig. 2, which contains three parts: the altitude profile $h(t)$, the velocity profile $V(t)$, and the path inclination profile $\gamma(t)$. From Table 1 and Fig. 2, the following comments arise:

Table 1 Optimal trajectory results

Quantity	Case 1	Case 2	Case 3	Units
h_0	120.0	120.0	120.0	km
V_0	9.040	9.905	10.310	km/s
γ	−3.034	−3.893	−4.204	deg
h_1	120.0	120.0	120.0	km
V_1	7.844	7.844	7.844	km/s
γ_1	0.319	0.319	0.319	deg
$h_{\min}$	79.50	76.35	75.36	km
PHR	35.90	59.61	72.70	W/cm^2
τ	2.147	2.297	2.347	ks
ΔV_{00}	1.025	1.445	1.490	km/s
ΔV_1	0.000	0.000	0.000	km/s
ΔV_{11}	0.025	0.025	0.025	km/s
ΔV	1.049	1.470	1.515	km/s

1) The optimal trajectory includes two branches: a relatively short descending flight branch (branch 1) and a long ascending flight branch (branch 2). As the HEO radius increases, the minimum altitude of the optimal trajectory decreases, implying that a deeper penetration into the atmosphere is required to ensure the proper amount of velocity depletion.

2) Velocity depletion takes place along the entire atmospheric trajectory but is concentrated mostly in the terminal part of branch 1 and the beginning part of branch 2.

3) The path inclination increases rapidly from the entry value (a few degrees negative) to zero value in branch 1, and it increases slowly from zero value to the exit value (a fraction of a degree positive) in branch 2.

4) The lift coefficient profile is nearly independent of the HEO radius. In branch 1, the lift coefficient decreases rapidly from the upper bound value to nearly the lower bound value; in branch 2, the lift coefficient stays near the lower bound value. See Fig. 2D of Ref. 17.

C. Guidance Implications

Consider the altitude-path inclination domain and, with reference to Fig. 2, regard the altitude profile $h = h(t)$ and the path inclination profile $\gamma = \gamma(t)$ as the parametric representation of the trajectory, the time t being the parameter. Upon elimination of the time, one obtains the path inclination-altitude relation $\gamma = \gamma(h)$. Then this relation can be rewritten in the normalized form $\theta = \theta(\eta)$, where θ and η denote normalized variables defined as follows:

$$\theta = \gamma/|\gamma_0|, \quad \text{branch 1} \tag{11a}$$

$$\theta = \gamma/|\gamma_0|, \quad \text{branch 2} \tag{11b}$$

and

$$\eta = (h_0 - h)/(h_0 - h_{\min}), \quad \text{branch 1} \tag{12a}$$

$$\eta = (h - h_{\min})/(h_0 - h_{\min}), \quad \text{branch 2} \tag{12b}$$

The normalized path inclination-altitude relation $\theta = \theta(\eta)$ is plotted in Fig. 3, which contains two parts: the descending flight branch (Fig. 3a) and the ascending flight branch (Fig. 3b). For branch 1, the normalized path inclination is nearly a linear function of the normalized altitude, and its slope is relatively steep; for branch 2, the normalized path inclination is also nearly a linear function of the normalized altitude, but its slope is relatively shallow. These observations are the basis of the gamma guidance law described in Sec. IV. This is a two-stage guidance law, designed as follows: for branch 1, the gamma guidance is a linear path inclination guidance; for branch 2, the gamma guidance is a constant path inclination guidance.

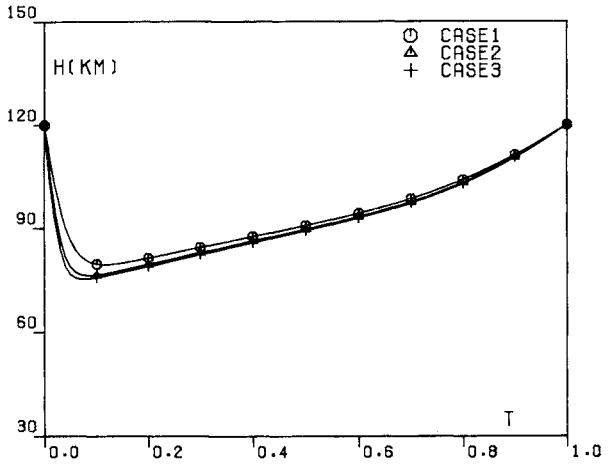

Fig. 2a Optimal trajectories, altitude h vs time t.

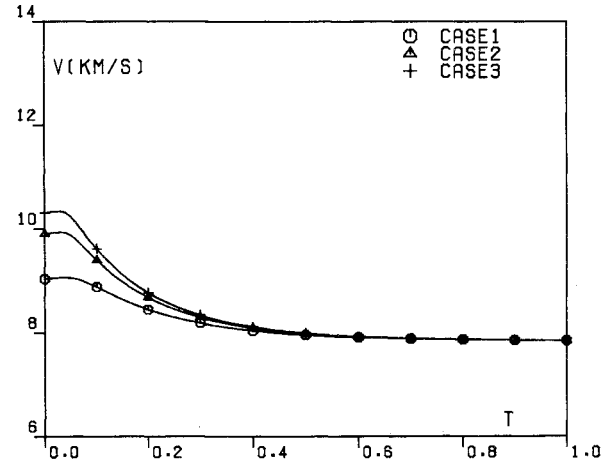

Fig. 2b Optimal trajectories, velocity V vs time t.

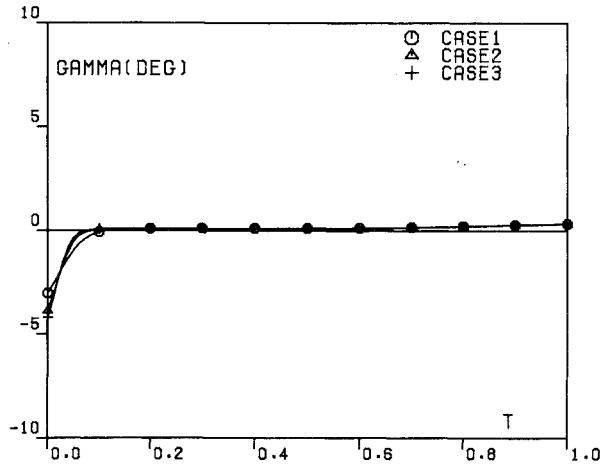

Fig. 2c Optimal trajectories, path inclination γ vs time t.

IV. Gamma Guidance Trajectories

In the previous section, optimal trajectories (OT) for coplanar AOT flight were determined. They include three phases: the preatmospheric phase, characterized by the velocity impulse ΔV_{00} at HEO; the atmospheric phase, characterized by a relatively short descending flight branch (branch 1) and a long ascending flight branch (branch 2); and the postatmospheric phase, characterized by the velocity impulse ΔV_1 at atmospheric exit and the velocity impulse ΔV_{11} at LEO.

In this section, we develop gamma guidance trajectories (GGT) for coplanar AOT flight under two basic requirements:

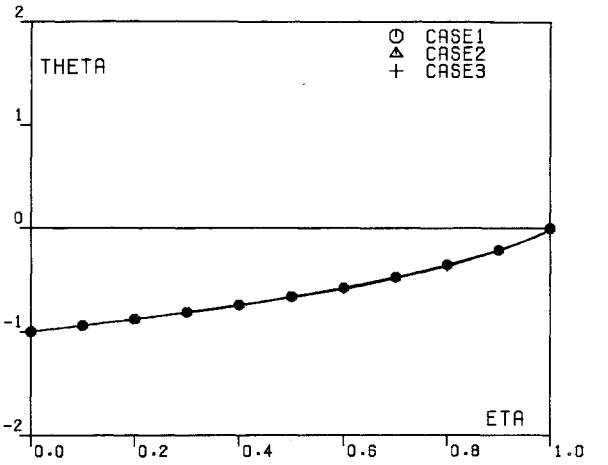

Fig. 3a Optimal trajectories, descending branch, normalized path inclination vs normalized altitude.

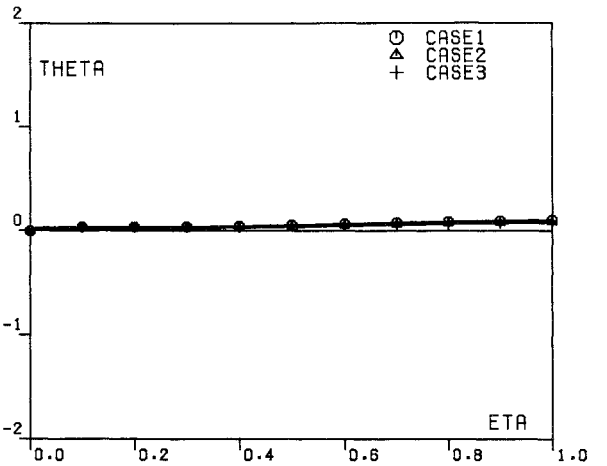

Fig. 3b Optimal trajectories, ascending branch, normalized path inclination vs normalized altitude.

1) the GGT should be close to the OT, and 2) the GGT should be simple, easy to implement, and reliable. First, we discuss the space portion of the GGT; then we discuss the atmospheric portion of the GGT.

A. Preatmospheric Phase

Initially, the spacecraft is in a high Earth orbit of radius r_{00}. To deorbit, the following velocity impulse is applied:

$$\Delta V_{00} = \sqrt{r_a/r_{00}}\, V_a - (r_a/r_{00}) V_0 \cos\gamma_0 \tag{13a}$$

with

$$V_0 = V_a\sqrt{2(r_{00}^2 - r_{00}r_a)/(r_{00}^2 - r_a^2\cos^2\gamma_0)} \tag{13b}$$

This enables the spacecraft to enter into an elliptical transfer orbit leading from HEO exit to atmospheric entry. In Eqs. (13), γ_0 is the entry path inclination and V_0 is the entry velocity. Because r_a, V_a are constant and r_{00} is given, Eqs. (13) imply that $V_0 = V_0(\gamma_0)$ and $\Delta V_{00} = \Delta V_{00}(\gamma_0)$. Hence, the selection of the entry angle γ_0 determines uniquely both the entry velocity V_0 and the initial velocity impulse ΔV_{00}.

B. Postatmospheric Phase

The postatmospheric phase includes two velocity impulses: a velocity impulse ΔV_1 at atmospheric exit and a velocity impulse ΔV_{11} at LEO entry.

Atmospheric Exit

The velocity impulse at atmospheric exit is determined with the relation

$$\Delta V_1 = \tilde{V}_1 - V_1 \tag{14a}$$

where

$$\tilde{V}_1 = V_a\sqrt{2(r_{11}^2 - r_{11}r_a)/(r_{11}^2 - r_a^2\cos^2\gamma_1)} \tag{14b}$$

This velocity impulse is essential for the GGT to compensate for previous velocity errors. In Eqs. (14), γ_1 is the exit path inclination, V_1 is the exit velocity before the velocity impulse, and $\tilde{V}_1$ is the exit velocity after the velocity impulse. Note that r_a, V_a are constant, r_{11} is given, and V_1, γ_1 are measured in actual flight.

LEO Entry

After the velocity impulse (14) is applied, the spacecraft enters into an elliptical transfer orbit leading from atmospheric exit to LEO entry. This elliptical transfer orbit is such that its apogee occurs at r_{11}. At this point, the velocity impulse ΔV_{11} is applied so as to achieve circularization into LEO. Specifically, ΔV_{11} is determined with the relation

$$\Delta V_{11} = \sqrt{r_a/r_{11}}V_a - V_{11} \tag{15}$$

in which V_{11} is the velocity at LEO entry before the velocity impulse. Note that r_a, V_a are constant, r_{11} is given, and V_{11} is measured in actual flight.

C. Atmospheric Phase

The atmospheric phase includes the descending flight branch (branch 1) and the ascending flight branch (branch 2). For both branches, a gamma guidance scheme is implemented in feedback control form. The switch from branch 1 to branch 2 is regulated by the switch velocity V_S, to be selected appropriately.

Descending Flight Branch

For branch 1, the gamma guidance is a linear path inclination guidance, which is implemented in the following feedback control form:

$$C_L - \tilde{C}_L(h, V, \gamma) = -K_1(\gamma - \tilde{\gamma}) \tag{16a}$$

$$\tilde{\gamma} = \gamma_0(h - h_T)/(h_0 - h_T) \tag{16b}$$

$$C_{La} \le C_L \le C_{Lb} \tag{16c}$$

Here, C_L is the instantaneous lift coefficient and $\tilde{C}_L$ is the nominal lift coefficient; C_{La} and C_{Lb} are the lower and upper bounds for the lift coefficient; γ is the instantaneous path inclination, $\tilde{\gamma}$ is the nominal path inclination, and γ_0 is the entry path inclination; h is the instantaneous altitude, h_0 is the entry altitude, and h_T is the target altitude; and K_1 is the gain coefficient for the path inclination error.

The feedback form (16) of the gamma guidance is strongly stable at the target altitude; this is because $\tilde{\gamma} < 0$ if $h > h_T$, while $\tilde{\gamma} > 0$ if $h < h_T$. In addition, it avoids overshooting and undershooting of the target altitude, since $\tilde{\gamma}$ varies smoothly between the entry value $\tilde{\gamma} = \gamma_0$ and the target altitude value $\tilde{\gamma} = 0$.

Ascending Flight Branch

For branch 2, the gamma guidance is a constant path inclination guidance, which is implemented via the following feedback control form:

$$C_L - \tilde{C}_L(h, V, \gamma) = -K_2(\gamma - \tilde{\gamma}) \tag{17a}$$

$$\tilde{\gamma} = \gamma_T \tag{17b}$$

$$C_{La} \le C_L \le C_{Lb} \tag{17c}$$

Here, γ_T denotes the target path inclination and K_2 is the gain coefficient for path inclination error.

Nominal Lift Coefficient

The nominal lift coefficient $\tilde{C}_L$ is computed with Eq. (1c) under the assumption of near-equilibrium conditions. Upon setting $\dot{\gamma} \cong 0$, invoking Eqs. (2) and (3), and observing that $\rho = \rho(h)$, $r = r(h)$, and $g = g(h)$, we obtain the relation

$$\tfrac{1}{2}C_L\rho(h)SV^2 + m[V^2/r(h) - g(h)]\cos\gamma = 0 \tag{18a}$$

which admits the solution

$$\tilde{C}_L = 2m[g(h) - V^2/r(h)]\cos\gamma/\rho(h)SV^2 \tag{18b}$$

which has the form $\tilde{C}_L = \tilde{C}_L(h, V, \gamma)$.

Gain Coefficients

The gain coefficients for path inclination error are given by

$$K_1 = \rho_*/\rho, \qquad K_2 = \rho_*/\rho \tag{19}$$

where $\rho = \rho(h)$ is the air density at the altitude h and $\rho_* = \rho(h_*)$ is the air density at the reference altitude $h_* = H/3 = 40$ km. This particular form of the gain coefficients is justified by the need for a more energetic control response at higher altitudes and a gentler control response at lower altitudes.

D. Guidance Parameters

The performance of the gamma guidance scheme depends on four parameters: the entry path inclination γ_0, the target altitude h_T of branch 1, the switch velocity V_S, and the target path inclination γ_T of branch 2. By proper selection of those parameters, the gamma guidance trajectory can be made close to the optimal trajectory. Extensive computer simulations show that the desirable values of the guidance parameters should be consistent with the following relations:

$$|\gamma_0|_{GGT} > |\gamma_0|_{OT} \tag{20a}$$

$$(h_T)_{GGT} < (h_{\min})_{OT} \tag{20b}$$

$$(V_s)_{GGT} = A(V_0)_{OT} + (1 - A)(V_1)_{OT}$$

$$= (V_1)_{OT} + A(V_0 - V_1)_{OT} \tag{20c}$$

$$(\gamma_T)_{GGT} = B(\gamma_1)_{OT} \tag{20d}$$

Inequality (20a) means that the entry path inclination of the GGT should be somewhat steeper than the entry path inclination of the OT.

Inequality (20b) means that the target altitude of the GGT should be somewhat lower than the minimum altitude of the OT.

Equation (20c) means that the switch velocity of the GGT should be a weighted average of the entry velocity of the OT and the exit velocity of the OT. The dimensionless constant A should be in a proper range.

Equation (20d) means that the target path inclination of the GGT should be some fraction of the exit path inclination of the OT. The dimensionless constant B should be in a proper range.

E. Numerical Results

The four guidance parameters γ_0, h_T, V_S, and γ_T were selected with the criteria of Sec. IVD, and the corresponding

Table 2 Gamma guidance trajectory parameters

Quantity	Case 1	Case 2	Case 3	Units
γ_0	−3.300	−4.100	−4.400	deg
h_T	78.25	75.75	74.32	km
V_S	8.700	9.180	9.400	km/s
γ_T	0.115	0.113	0.114	deg

Table 3 OT, GGT, and MGGT results, case 3 (no dispersion)

Quantity	OT	GGT	MGGT	Units
h_0	120.0	120.0	120.0	km
V_0	10.310	10.310	10.310	km/s
γ_0	−4.204	−4.400	−4.500	deg
h_1	120.0	120.0	120.0	km
V_1	7.844	7.841	7.835	km/s
γ_1	0.319	0.300	0.245	deg
$h_{\min}$	75.36	74.28	71.14	km
PHR	72.70	78.27	96.97	W/cm^2
τ	2.347	2.405	3.012	ks
ΔV_{00}	1.490	1.490	1.491	km/s
ΔV_1	0.000	0.003	0.011	km/s
ΔV_{11}	0.025	0.024	0.022	km/s
ΔV	1.515	1.517	1.523	km/s

Table 4 GGT and MGGT parameters, case 3 (no dispersion)

Quantity	GGT	MGGT	Units
γ_0	−4.400	−4.500	deg
h_T	74.32	71.14	km
V_S	9.400	8.400	km/s
γ_T	0.114	0.150	deg

guidance trajectories were computed. Table 2 shows the combinations of guidance parameters used for cases 1, 2, and 3. The resulting GGT is geometrically close to the corresponding OT, so as to retain the good features of the OT concerning the total characteristic velocity

$$\Delta V = \Delta V_{00} + \Delta V_1 + \Delta V_{11} \tag{21}$$

and the peak heating rate.

For a particular case (namely, case 3, GEO-to-LEO transfer), Table 3 compares the results obtained for the OT and the GGT, while Fig. 4 compares the altitude profiles $h(t)$ of the OT and the GGT.

For detailed information about the behavior of the GGT, see Ref. 17.

V. Modified Gamma Guidance Trajectories

In real AOT flights, there are dispersion effects arising from navigation errors, variations of the atmospheric density, and uncertainties in the aerodynamic coefficients. Navigation errors refer to the space portion of AOT flights and induce errors in the entry path inclination; density variations are due to such factors as latitude, season, time of the day or the night, and solar activity or are due to lack of sufficient knowledge of a particular planetary atmosphere (Mars); uncertainties in the aerodynamic coefficients arise because wind-tunnel tests might not simulate precisely the combination of high speeds and low densities characterizing AOT flights or arise because computational fluid dynamics schemes might not account precisely for all of the physical factors involved.

While the gamma guidance scheme of Sec. IV yields a trajectory close to the optimal trajectory in the absence of dispersion effects, that scheme is not sufficiently robust with respect to large parameter dispersion. In this connection, there are two ways for improving the stability of the gamma guidance scheme: 1) to decrease the target altitude, while simultaneously increasing the modulus of the entry path inclination; and 2) to adjust the switch velocity and the target path inclination by means of a predictor-corrector algorithm. The resulting trajectory is called modified gamma guidance trajectory (MGGT).

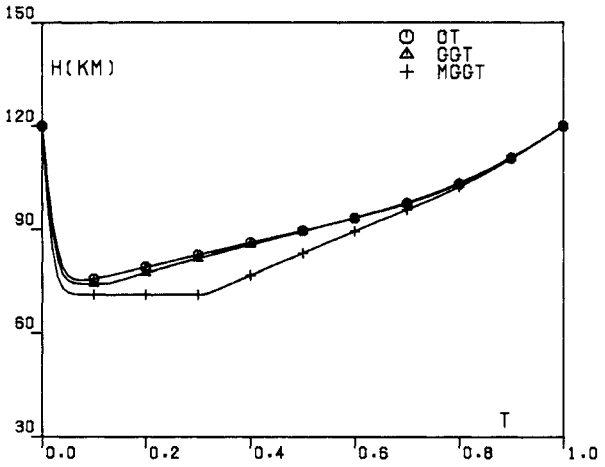

Fig. 4 Trajectory comparison, case 3, altitude h vs time t.

We note that the relations (20) governing the gamma guidance are also valid for the modified gamma guidance if the subscript GGT is replaced with the subscript MGGT. However, an important difference must be stressed. In the gamma guidance, the four parameters (γ_0, h_T, V_S, γ_T) are preselected. In the modified gamma guidance, two parameters (γ_0, h_T) are preselected, while the remaining parameters (V_S, γ_T) are adjusted in flight with the predictor-corrector algorithm. With reference to the relations (20), this is the same as stating that the dimensionless quantities A, B behave as constants in the gamma guidance but as parameters in the modified gamma guidance.

For the details of the predictor-corrector algorithm, see Ref. 17. Here, it suffices to say that the predictor-corrector algorithm is started at the target altitude by assuming some typical values for the pair (A,B), hence some typical values for the pair (V_S, γ_T). Then, for branch 2, Eqs. (1-3) are integrated in forward time using the feedback control form (17) of the constant path inclination guidance. Once the state of the spacecraft is known at atmospheric exit, one verifies compliance with the inequality

$$\Delta V_1 \leq 0.03 \text{ km/s} \tag{22}$$

If inequality (22) is satisfied, the assumed pair (A,B) is accepted, and the predictor-corrector procedure is terminated. If inequality (22) is violated, one performs two successive one-dimensional searches in the (A,B) plane. The search is terminated whenever a pair (A,B) is found such that inequality (22) is satisfied, subject to suitable safeguards. For details, see Ref. 17.

Numerical Results

With reference to case 3, GEO-to-LEO transfer, we report here on a comparative study of the GGT and the MGGT in the absence of dispersion effects. Dispersion effects are discussed separately in Sec. VI.

Table 3 compares the results obtained for the GGT and the MGGT, while Table 4 presents typical combinations of the guidance parameters for both the GGT and the MGGT. Figure 4 presents a graphical comparison of the altitude profiles of the GGT and the MGGT.

For details on the behavior of the MGGT, see Ref. 17.

Table 5 Dispersion effects, MGGT, case 3

Dispersion factor	γ_0, deg	h_T, km	V_S, km/s	γ_T, deg	PHR, W/cm^2	τ, ks	ΔV, km/s
$F_{\gamma 0} = 0.91$	− 4.1	71.14	8.40	0.15	83.79	2.986	1.523
$F_{\gamma 0} = 1.00$	− 4.5	71.14	8.40	0.15	96.97	3.012	1.523
$F_{\gamma 0} = 1.44$	− 6.5	71.14	8.40	0.15	180.80	2.810	1.529
$F_\rho = 0.33$	− 4.5	62.98	8.40	0.15	87.66	3.670	1.535
$F_\rho = 1.00$	− 4.5	71.14	8.40	0.15	96.97	3.012	1.523
$F_\rho = 10.00$	− 4.5	85.84	8.40	0.15	127.67	2.376	1.519
$F_{CD0} = 0.10$	− 4.5	71.14	8.20	0.15	98.96	4.268	1.547
$F_{CD0} = 1.00$	− 4.5	71.14	8.40	0.15	96.97	3.012	1.523
$F_{CD0} = 5.00$	− 4.5	71.14	9.10	0.21	90.00	1.953	1.534
$F_K = 0.10$	− 4.5	71.14	8.15	0.15	103.63	4.281	1.523
$F_K = 1.00$	− 4.5	71.14	8.40	0.15	96.97	3.012	1.523
$F_K = 5.00$	− 4.5	71.14	9.10	0.25	83.95	1.646	1.541
$F_{CLR} = 0.33$	− 4.5	62.98	9.00	0.15	174.29	2.390	1.555
$F_{CLR} = 1.00$	− 4.5	71.14	8.40	0.15	96.97	3.012	1.523
$F_{CLR} = 3.00$	− 4.5	78.41	8.40	0.15	49.08	2.571	1.533

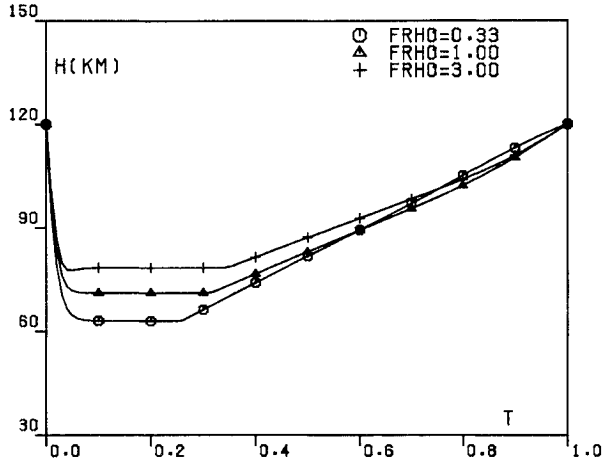

Fig. 5 Effect of density change, MGGT, case 3, altitude h vs time t.

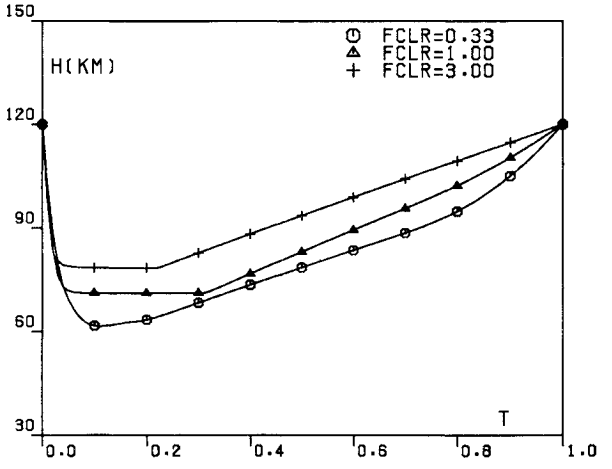

Fig. 6 Effect of change in the lift range, MGGT, case 3, altitude h vs time t.

VI. Dispersion Effects

Here we report on the behavior of the MGGT vis-a-vis dispersion effects due to navigation errors, variations of the atmospheric density, and uncertainties in the aerodynamic coefficients. For the sake of discussion, let unprimed quantities denote standard values; let primed quantities denote dispersed values; and let the following dispersion factors be defined:

$$F_{\gamma 0} = \gamma_0'/\gamma_0 \tag{23a}$$

$$F_\rho = \rho'(h)/\rho(h) \tag{23b}$$

$$F_{CD0} = C_{D0}'/C_{D0} \tag{23c}$$

$$F_K = K'/K \tag{23d}$$

$$F_{CLR} = (C_{Lb}' - C_{La}')/(C_{Lb} - C_{La}) \tag{23e}$$

Here, $F_{\gamma 0}$ is the entry path inclination factor; F_ρ is the density factor; F_{CD0} is the zero-lift drag factor; F_K is the induced drag factor; and F_{CLR} is the lift range factor. Note that the factors (23) are defined in such a way that they are equal to one in the absence of dispersion effects, while they are different from one in the presence of dispersion effects.

It is of interest to determine the range of values of the dispersion factors (23) for which the MGGT can execute safely the atmospheric pass. With reference to case 3, GEO-to-LEO transfer, extensive computer simulations lead to the following stability range for the dispersion factors:

$$0.91 \le F_{\gamma 0} \le 1.44 \tag{24a}$$

$$0.33 \le F_\rho \le 10.00 \tag{24b}$$

$$0.10 \le F_{CD0} \le 5.00 \tag{24c}$$

$$0.10 \le F_K \le 5.00 \tag{24d}$$

$$0.33 \le F_{CLR} \le 3.00 \tag{24e}$$

The following comments are pertinent:

1) Concerning the path inclination factor $F_{\gamma 0}$, note that the stability range (24a) corresponds to $+0.4 \ge \Delta\gamma_0 \ge -2.0$ deg, where $\Delta\gamma_0 = \gamma_0' - \gamma_0$.

2) Concerning the density factor F_ρ, note that its value has been assumed constant, independent of the altitude. The case where F_ρ depends on the altitude is treated separately.

3) Table 5 supplies the values of the guidance parameters γ_0, h_T, V_S, and γ_T plus the peak heating rate PHR, the flight time τ, and the characteristic velocity ΔV. From inequalities (24) and Table 5, it appears that the modified gamma guidance trajectory is quite stable with respect to dispersion factors arising from navigation errors, variations of the atmospheric density, and uncertainties in the aerodynamic coefficients.

4) Reference 17 contains a detailed analysis of the behavior of the modified gamma guidance trajectory vis-a-vis dis-

persion effects. Here, by way of example, we show in Figs. 5 and 6 the effects of the dispersion factors F_ρ and F_{CLR} on the altitude profile $h(t)$.

Variable Dispersion Factor

With reference to the density dispersion factor F_ρ, it is known from Space Shuttle re-entry analyses (e.g., STS-6) that such a dispersion factor might be altitude dependent. To reproduce in a simple way this situation, the following variable dispersion factor is now considered:

$$F_\rho = 1 + C \sin[(\pi/2)(h - h_{**})/(h_0 - h_{**})] \tag{25}$$

where $h_0 = 120$ km and $h_{**} = 80$ km. Clearly, the constant C must be chosen in the range $-1 < C < +1$.

With reference to case 3, GEO-to-LEO transfer, computer simulations show that the MGGT is stable in the range

$$-0.8 \leq C \leq +0.8 \tag{26}$$

Note that inequality (26) covers the range of systematic variability of the density around that of the US Standard Atmosphere, 1976 (Ref. 13, page 25, Fig. 26).

VII. Conclusions

With reference to the optimization and guidance of trajectories for coplanar, aeroassisted orbital transfer, the following major conclusions are obtained:

1) The optimal trajectories include two branches: a relatively short descending flight branch (branch 1) and a long ascending flight branch (branch 2). In branch 1, the path inclination is nearly a linear function of the altitude; in branch 2, the path inclination is a slowly varying function of the altitude.

2) Gamma guidance trajectories are developed. They employ a feedback control scheme in which the lift coefficient is adjusted according to a two-stage gamma guidance law. For branch 1, the gamma guidance is a linear path inclination guidance; for branch 2, the gamma guidance is a constant path inclination guidance. By properly selecting four guidance parameters (the entry path inclination, the target altitude, the switch velocity, and the target path inclination), the gamma guidance trajectory can be made close to the optimal trajectory.

3) Improvements in stability are possible via a modified gamma guidance, which differs from the gamma guidance in two aspects: lower target altitude, coupled with steeper entry path inclination; and use of a predictor-corrector algorithm to adjust the values of the switch velocity and the target path inclination. Computer simulations show that the modified gamma guidance trajectory is quite stable with respect to dispersion effects arising from navigation errors, variations of the atmospheric density, and uncertainties in the aerodynamic coefficients.

4) A byproduct of the dispersion studies is the following design concept. For coplanar, aeroassisted orbital transfer, the lift-range-to-weight ratio appears to play a more important role than the lift-to-drag ratio. This is because the lift-range-to-weight ratio controls mainly the minimum altitude (hence, the peak heating rate) of the guidance trajectory; on the other hand, the lift-to-drag ratio controls mainly the duration of the atmospheric pass of the guidance trajectory.

Acknowledgments

This research was supported by Jet Propulsion Laboratory Contract 956415, by NASA Marshall Space Flight Center Grant NAG-8-820, and by Texas Advanced Technology Program Grant TATP-003604020.

References

[1]Mease, K. D., and Vinh, N. X., "Minimum-Fuel Aeroassisted Coplanar Orbit Transfer Using Lift Modulation," *Journal of Guidance, Control, and Dynamics,* Vol. 8, No. 1, 1985, pp. 134–141.

[2]Miele, A., Basapur, V. K., and Mease, K. D., "Nearly-Grazing Optimal Trajectories for Aeroassisted Orbital Transfer," *Journal of the Astronautical Sciences,* Vol. 34, No. 1, 1986, pp. 3–18.

[3]Miele, A., Basapur, V. K., and Lee, W. Y., "Optimal Trajectories for Aeroassisted, Coplanar Orbital Transfer," *Journal of Optimization Theory and Applications,* Vol. 52, No. 1, 1987, pp. 1–24.

[4]Mease, K. D., "Optimization of Aeroassisted Orbital Transfer: Current Status," *Journal of the Astronautical Sciences,* Vol. 36, Nos. 1–2, 1988, pp. 7–33.

[5]Miele, A., Wang, T., Lee, W. Y., and Zhao, Z. G., "Optimal Trajectories for the Aeroassisted Flight Experiment," IAF Paper 89-361, 40th Congress of the International Astronautical Federation, Malaga, Spain, 1989.

[6]Vinh, N. X., Johannesen, J. R., Mease, K. D., and Hanson, J. M., "Explicit Guidance of Drag-Modulated Aeroassisted Transfer Between Elliptical Orbits," *Journal of Guidance, Control, and Dynamics,* Vol. 9, No. 3, 1986, pp. 274–280.

[7]Mease, K. D., and McCreary, F. A., "Atmospheric Guidance Law for Planar Skip Trajectories," 12th Atmospheric Flight Mechanics Conference, Snowmass, CO, AIAA Paper 85-1818, Aug. 1985.

[8]Lee, B. S., and Grantham, W. J., "Aeroassisted Orbital Maneuvering Using Lyapunov Optimal Feedback Control," *Journal of Guidance, Control, and Dynamics,* Vol. 12, No. 2, 1989, pp. 237–242.

[9]Gamble, J. D., Cerimele, C. J., Moore, T. E., and Higgins, J., "Atmospheric Guidance Concepts for an Aeroassist Flight Experiment," *Journal of the Astronautical Sciences,* Vol. 36, Nos. 1–2, 1988, pp. 45–71.

[10]Miele, A., Wang, T., and Lee, W. Y., "Optimization and Guidance of Trajectories for Coplanar, Aeroassisted Orbital Transfer," Rice Univ., Aero-Astronautics Rept. 241, Houston, TX, 1989.

[11]Miele, A., Wang, T., Tzeng, C. Y., and Melvin, W. W., "Abort Landing Guidance Trajectories in the Presence of Windshear," *Journal of the Franklin Institute,* Vol. 326, No. 2, 1989, pp. 185–220.

[12]Miele, A., Wang, T., Melvin, W. W., and Bowles, R. L., "Acceleration, Gamma, and Theta Guidance for Abort Landing in a Windshear," *Journal of Guidance, Control, and Dynamics,* Vol. 12, No. 6, 1989, pp. 815–821.

[13]NOAA, NASA, and USAF, "US Standard Atmosphere, 1976," U.S. Government Printing Office, Washington, DC, 1976.

[14]Miele, A., Wang, T., and Basapur, V. K., "Primal and Dual Formulations of Sequential Gradient-Restoration Algorithms for Trajectory Optimization Problems," *Acta Astronautica,* Vol. 13, No. 8, 1986, pp. 491–505.

[15]Miele, A., and Wang, T., "Primal-Dual Properties of Sequential Gradient-Restoration Algorithms for Optimal Control Problems, Part 1, Basic Problem," *Integral Methods in Science and Engineering,* edited by F. R. Payne et al., Hemisphere, Washington, DC, 1986, pp. 577–607.

[16]Miele, A., and Wang, T., "Primal-Dual Properties of Sequential Gradient-Restoration Algorithms for Optimal Control Problems, Part 2, General Problem," *Journal of Mathematical Analysis and Applications,* Vol. 119, Nos. 1–2, 1986, pp. 21–54.

[17]Miele, A., and Wang, T., "Gamma Guidance of Trajectories for Coplanar, Aeroassisted Orbital Transfer," Rice Univ., Aero-Astronautics Rept. 246, Houston, TX, 1990.